

Cover Page



Universiteit Leiden



The handle <http://hdl.handle.net/1887/25711> holds various files of this Leiden University dissertation

**Author:** Ramkisoensing, Arti Anushka

**Title:** Molecular and environmental cues in cardiac differentiation of mesenchymal stem cells

**Issue Date:** 2014-05-07

## CHAPTER II

# HUMAN EMBRYONIC AND FETAL MESENCHYMAL STEM CELLS DIFFERENTIATE TOWARD THREE DIFFERENT CARDIAC LINEAGES IN CONTRAST TO THEIR ADULT COUNTERPARTS

*Arti A. Ramkisoensing<sup>a</sup>, Daniël A. Pijnappels<sup>a</sup>, Saïd F.A. Askar<sup>a</sup>, Robert Passier<sup>b</sup>, Jim Swildens<sup>a,c</sup>, Marie José Goumans<sup>c</sup>, Cindy I. Schutte<sup>a</sup>, Antoine A.F. de Vries<sup>a</sup>, Sicco Scherjon<sup>d</sup>, Christine L. Mummery<sup>b</sup>, Martin J. Schalij<sup>a</sup>, Douwe E. Atsma<sup>a</sup>.*

<sup>a</sup>Departments of Cardiology, <sup>b</sup>Embryology and Anatomy, <sup>c</sup>Molecular Cell Biology, <sup>d</sup>Obstetrics and Gynaecology, Leiden University Medical Center, 2300 RC Leiden, The Netherlands.

*PLoS One. 2011;6(9):e24164.*

**ABSTRACT**

Mesenchymal stem cells (MSCs) show unexplained differences in differentiation potential. In this study, differentiation of human (h) MSCs derived from embryonic, fetal and adult sources toward cardiomyocytes, endothelial and smooth muscle cells was investigated.

Labeled hMSCs derived from embryonic stem cells (hESC-MSCs), fetal umbilical cord, bone marrow, amniotic membrane and adult bone marrow and adipose tissue were co-cultured with neonatal rat cardiomyocytes (nrCMCs) or cardiac fibroblasts (nrCFBs) for 10 days, and also cultured under angiogenic conditions.

Cardiomyogenesis was assessed by human-specific immunocytological analysis, whole-cell current-clamp recordings, human-specific qRT-PCR and optical mapping. After co-culture with nrCMCs, significantly more hESC-MSCs than fetal hMSCs stained positive for  $\alpha$ -actinin, whereas adult hMSCs stained negative. Furthermore, functional cardiomyogenic differentiation, based on action potential recordings, was shown to occur, but not in adult hMSCs. Of all sources, hESC-MSCs expressed most cardiac-specific genes. hESC-MSCs and fetal hMSCs contained significantly higher basal levels of connexin43 than adult hMSCs and co-culture with nrCMCs increased expression. After co-culture with nrCFBs, hESC-MSCs and fetal hMSCs did not express  $\alpha$ -actinin and connexin43 expression was decreased. Conduction velocity (CV) in co-cultures of nrCMCs and hESC-MSCs was significantly higher than in co-cultures with fetal or adult hMSCs. In angiogenesis bioassays, only hESC-MSCs and fetal hMSCs were able to form capillary-like structures, which stained for smooth muscle and endothelial cell markers.

Human embryonic and fetal MSCs differentiate toward three different cardiac lineages, in contrast to adult MSCs. Cardiomyogenesis is determined by stimuli from the cellular microenvironment, where connexin43 may play an important role.

## INTRODUCTION

Despite significant advances in the management of cardiovascular disease, it remains the predominant cause of morbidity and mortality in Western countries [1]. The risk of developing cardiovascular disease increases with age and is associated with progressive impairment of cardiovascular repair mechanisms, including the capacity of the heart to replace damaged cells [2].

In recent years, cell therapy has been studied intensively as novel therapeutic option for cardiac diseases. After transplantation and engraftment of cells in the host myocardium, different mechanisms are thought to be responsible for the improvement in cardiac function, including angiogenesis and cardiomyogenesis [3]. Mesenchymal stem cells (MSCs) are one of the cell types studied in clinical trials for treatment of ischemic heart disease. However, MSCs themselves are prone to the effects of aging and disease and if autologous MSCs are used, may suffer from decreased ability to proliferate, differentiate, home, engraft and exert immunosuppressive effects [4,5]. Moreover, the developmental stage of tissues and different states of disease alter the microenvironmental regulation of stem cell behaviour [6]. Whether the developmental stage of MSC donor tissue also affects the cardiac differentiation potential of MSCs is not completely understood. While the role of MSCs in cardiac development is largely unknown, several studies indicate that MSCs derived from young cell sources, like umbilical cord blood, appear to retain their primitive characteristics [7,8]. Also, some of these MSCs seem to possess cardiovascular differentiation potential *in vitro* and *in vivo* [9,10]. More recently, cells with MSC-like characteristics have been derived from human embryonic stem cells (ESCs) [11–15]. These cells resemble hMSCs derived from various tissue sources with respect to morphology, surface marker profile, immunogenicity and differentiation potential toward osteogenic, adipogenic and chondrogenic lineages [12,14]. More important, they lack expression of pluripotency-associated markers, and after transplantation, no teratoma formation has been reported [12,16]. MSCs derived from human ESCs may therefore be mesoderm progenitors like primitive MSCs and may constitute the most primitive committed mesodermal cell type.

In this study, it was investigated whether the developmental stage of the tissue, from which hMSCs were derived, had an effect on the cardiac differentiation potential of these cells. To this end, the ability of hMSCs derived from ESCs, fetal (amniotic membrane, umbilical cord and bone marrow) and adult (adipose tissue and bone marrow) tissue sources to differentiate towards cardiomyocytes, smooth muscle cells and endothelial cells was studied.

## **MATERIALS AND METHODS**

### **ISOLATION AND CULTURE OF NEONATAL RAT CARDIOMYOCYTES AND FIBROBLASTS**

All animal experiments were approved by the Animal Experiments Committee of the Leiden University Medical Center (LUMC) and conform to the Guide for the Care and Use of Laboratory Animals, as stated by the US National Institutes of Health (permit numbers: 09012 and 10236). Neonatal rat ventricular cardiomyocytes (nrCMCs) and fibroblasts (nrCFBs) were isolated and cultured as described previously [10].

### **ISOLATION, CULTURE AND CHARACTERIZATION OF hMSCS**

All human-derived tissues were collected based on individual written (parental) informed consent, after approval by the Medical Ethics committee of the LUMC, where all investigations were performed. The investigation conforms with the principles outlined in the Declaration of Helsinki. Human mesenchymal stem cells (hMSCs) were derived from embryonic stem cells (hESC-MSCs), fetal amniotic membrane (amniotic), umbilical cord (UC), bone marrow (BM), adult BM and adipose tissue (adipose). Furthermore, fetal human skin fibroblasts (hSFBS) were also isolated and used as control cells (see Online Supplement for extensive description of cell isolation and culture procedures). All hMSCs were characterized by flow cytometry, adipogenic and osteogenic differentiation ability, immunocytological analyses, growth kinetics and telomere length. After characterization, cells were labeled with enhanced green fluorescent protein (eGFP) and put in co-culture with nrCMCs or nrCFBs for 10 days to study their cardiomyogenic differentiation potential. Differentiation was assessed by human-specific immunocytological analyses, whole-cell current-clamp recordings, human-specific quantitative reverse transcription-polymerase chain reaction (qRT-PCR) analysis and optical mapping of action potential propagation. In addition, Western Blot analysis was used to study the expression of connexin43 (Cx43) in relation to differentiation of hMSCs. All experiments described below were conducted using hMSCs from passage 3-6.

### **FLOW CYTOMETRY**

Analysis of surface marker expression was carried out by flow cytometry using fluorescein isothiocyanate-, phycoerythrin- or allophycocyanin-conjugated antibodies directed against human CD105 (Ansell, Bayport, MN, USA), CD90, CD73, CD45, CD34, CD31, CD24 and stage-specific embryonic antigen-4 (SSEA-4) (all from Becton Dickinson, Franklin Lakes, NJ, USA).

### **ADIPOGENIC AND OSTEOGENIC DIFFERENTIATION**

Adipogenesis and osteogenesis of hMSCs were induced by incubating hMSCs in appropriate differentiation media. Lipid accumulation was assessed by Oil Red O

(Sigma-Aldrich, St. Louis, MO, USA), while calcium deposits were visualized by staining the cells with 2% Alizarine Red S (Sigma-Aldrich).

#### **GROWTH KINETICS**

Growth kinetics of the hMSCs was analyzed by calculating population doublings (PDs). hMSCs were plated in triplicate and trypsinized every 5 days and subjected to Trypan Blue staining to determine the viable cell concentration using a hemocytometer.

#### **RELATIVE TELOMERE LENGTH**

Genomic DNA from experimental and reference samples was obtained using DNAzol (Invitrogen, Breda, The Netherlands). Relative telomere lengths were measured by SYBR Green-based (Qiagen, Valencia, CA, USA) qRT-PCR amplification of telomere repeats (T) and single-copy gene *36B4* (S) in a LightCycler 480 Real-Time PCR System (Roche, Foster City, CA, USA).

#### **IMMUNOCYTOCHEMICAL ANALYSES**

Co-cultures or monocultures were fixed in 4% paraformaldehyde, permeabilized with 0.1% Triton X-100, and stained with primary antibodies. Primary antibodies specific for human lamin A/C (Vector laboratories, Burlingame, CA, USA), SSEA-4, Oct3/4 (both Santa Cruz Biotechnologies, Santa Cruz, CA, USA), Nanog (R&D Systems, Minneapolis, MN, USA), CD90, CD73, and CD105 were used to characterize hESC-MSCs. Co-cultures were stained with  $\alpha$ -actinin, Cx43 (both Sigma-Aldrich) and human lamin A/C. Primary antibodies were visualized with Alexa fluor-conjugated antibodies (Invitrogen). Nuclei were stained using Hoechst 33342 (Invitrogen). A fluorescence microscope equipped with a digital camera (Nikon Eclipse, Nikon Europe, Badhoevedorp, The Netherlands) and dedicated software (Image-Pro Plus, Version 4.1.0.0, Media Cybernetics, Silver Spring, MD, USA) were used to analyze data. All cultures were treated equally using the same antibody dilutions and exposure times.

#### **ELECTROPHYSIOLOGICAL MEASUREMENTS IN PHARMACOLOGICALLY UNCOUPLED HMSCS IN CO-CULTURE WITH NRCMCS**

In order to study functional cardiomyogenic differentiation in hMSCs, either eGFP-labeled fetal or adult hMSCs were put in co-culture with nrCMCs and studied as described previously [10]. In brief, at day 10 of co-culture, 180  $\mu$ mol/L of 2-aminoethoxydiphenyl borate (2-APB) (Tocris, Ballwin, MO, USA) was added to the extracellular solution, resulting in gap junction uncoupling [17,18], which allowed for single-cell studies within the co-culture. Next, whole-cell current-clamp recordings were performed in eGFP-labeled hMSCs.

**HUMAN-SPECIFIC QUANTITATIVE REVERSE TRANSCRIPTION PCR**

Total cellular RNA was extracted from monocultures of hMSCs and from co-cultures consisting of hMSCs and nrCMCs using the RNeasy Mini kit (Qiagen). Oligo (dT)-primed reverse transcription was performed on 2 µg of total cellular RNA and the resultant cDNA was used for PCR amplification using SYBR Green. To detect changes in cardiac and pluripotency gene expression levels, only human-specific primers were used. The expression of the genes of interest was normalized to that of the housekeeping gene *glyceraldehyde-3-phosphate dehydrogenase* (GAPDH). Specific primer information and annealing temperatures are provided in the Online Supplement. Data were analyzed using the  $\Delta$ Ct method.

**OPTICAL MAPPING TO DETERMINE CONDUCTION VELOCITY IN CO-CULTURES OF NRCMCS AND DIFFERENT TYPES OF HMSCS**

Action potential conduction velocity (CV) was investigated on a whole-culture scale in wells of a 24-well plate by optically mapping using the voltage-sensitive dye di-4-ANEPPS (Invitrogen). The measurements were performed 10 days after seeding of either  $8 \times 10^5$  nrCMCs (nrCMC monoculture) or  $8 \times 10^5$  nrCMCs plus  $8 \times 10^4$  nrCFBs or  $8 \times 10^4$  hMSCs (nrCMC/nrCFB or nrCMC/hMCS co-cultures) per well. The co-cultures were mapped using the Ultima-L optical mapping setup (SciMedia, Costa Mesa, CA, USA). Optical signal recordings were analyzed using Brain Vision Analyze 0909 (Brainvision Inc, Tokyo, Japan). The CV of all (co-)cultures was determined in a blinded manner.

**ASSESSMENT OF ANGIOGENESIS**

All types of hMSCs were plated on Matrigel (Becton Dickinson) and cultured in Endothelial Growth Medium-2 (Cambrex IEP, Wiesbaden, Germany) containing 100 ng/mL recombinant human VEGF-A<sub>165</sub> (R&D Systems) up to 24 h to determine their ability to form capillary-like structures. Following culture under angiogenic conditions, cells were fixed and stained with antibodies specific for smooth muscle myosin heavy chain (smMHC; Sigma-Aldrich) and platelet/endothelial cell adhesion molecule-1 (PECAM-1; Santa Cruz).

**WESTERN BLOT ANALYSIS**

Homogenates were made from at least 5 different isolations of hMSCs per source. Equal amounts of protein were size-fractionated in a 12% NuPage Tris-Acetate gel (Invitrogen) and transferred to a Hybond-P PVDF membrane (GE Healthcare, Waukesha, WI, USA). This membrane was incubated for 1 h with an antibody against Cx43 followed by incubation with horse radish peroxidase conjugated goat anti-rabbit secondary antibody (Santa Cruz). To check for equal protein loading, the housekeeping protein GAPDH (Chemicon International, Temecula, CA, USA) was used.

## STATISTICS

Experimental results were expressed as mean±standard deviation (SD) for a given number (n) of observations. Data was analyzed by Student's t-test for direct comparisons. Analysis of variance followed by the appropriate post-hoc analysis was performed for multiple comparisons. Statistical analysis was performed using SPSS 16.0 for Windows (SPSS Inc, Chicago, IL, USA). Differences were considered statistically significant at  $P<0.05$ .

A detailed description of the materials and methods can be found in the Supplemental Materials and Methods S1.

## RESULTS

### ISOLATION AND CHARACTERIZATION OF HMSCS

All types of hMSCs displayed a spindle-shaped morphology (Supplemental Figure S1A1-F1). To evaluate MSC properties, their surface phenotype and adipogenic and osteogenic differentiation capacity were studied. All types of hMSCs were negative for CD31 (endothelial cell marker), CD34, CD45 (hematopoietic cell markers), and SSEA-4 (embryonic stem cell marker), whereas they were positive for CD90, CD73 and CD105 (mesenchymal cell markers). Furthermore, hESC-MSCs were negative for CD24, indicating absence of hESCs in our cultures (Supplemental Table S1). *In vitro* differentiation assays confirmed that all types of hMSCs were able to differentiate into adipocytes and osteoblasts thus confirming their multipotent differentiation potential (Supplemental Figure S1A2-F2 and S1A3-F3, respectively).

### GROWTH KINETICS

Comparison of the growth kinetics of hESC-MSCs with those of fetal or adult hMSCs showed that hESC-MSCs had a significantly larger replication capacity during 20 days in culture (35.1 PDs) than any of the fetal hMSCs types (22.3-31.6 PDs) and both types of adult MSCs (6.4-12.8 PDs) ( $P<0.001$ ). Fetal hMSCs also proliferated more rapidly and grew to higher densities than both types of adult hMSCs ( $P<0.001$ ) (Supplemental Figure S1G).

### TELOMERE LENGTH

Replicative stability of hMSCs was determined by estimating their relative telomere lengths (i.e. telomere repeat copy number to single gene copy number [T/S] ratio). Relative telomere length was significantly longer in hESC-MSCs ( $4.87\pm 0.7$ ) and in fetal hMSCs ( $2.48\pm 0.4$ ) than in adult hMSCs ( $0.89\pm 0.2$ ) ( $P<0.05$ ;  $n=10$  samples from different isolations for each hMSC group). Relative telomere length was also

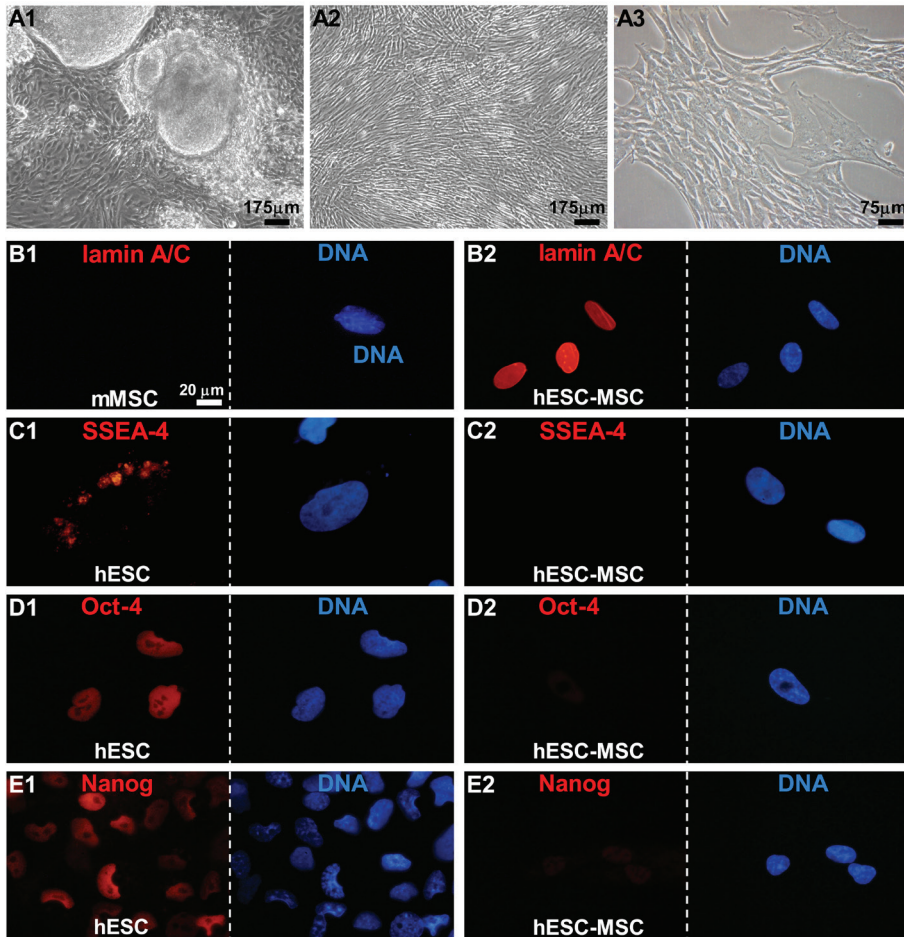


**Figure 1.** Characterization of hESC-MSCs: (A1) Bright field image of a hESC colony in which the cells at the periphery are differentiating toward spindle-shaped fibroblast-like cells and (A2-A3) pure cultures of hESC-MSC. (B1-B2) Confirmation of the human origin of the hMSCs derived from hESC colonies with the aid of a human-specific lamin A/C antibody. Incubation of murine MSCs (mMSCs; negative control cells) with this antibody (B1) did not produce signal corroborating its species specificity. (C1-E2) Immunostaining of hESC colonies and hMSCs derived from these colonies for the embryonic stem cell marker SSEA-4 and the pluripotency markers Oct-4 and Nanog. Nuclei were detected with Hoechst.

significantly longer in hESC-MSCs than in fetal hMSCs ( $P < 0.05$ ;  $n = 10$  samples from different isolations for each hMSC group) (Supplemental Figure S1H).

#### IMMUNOCYTOLOGICAL CHARACTERIZATION OF HESC-MSCS

All fibroblast-like cells derived from the hESC colonies (Figure 1A1-A3) were recognized by a monoclonal antibody specific for human lamin A/C confirming the human origin of these cells (Figure 1B2). Murine MSCs (mMSCs), which served as a negative control, were negative for this marker (Figure 1B1). In addition, hESC-MSCs were negative for the undifferentiated hESC marker SSEA-4 and the pluripotency markers Oct-4 and Nanog (Figure 1C2-E2) in contrast to the hESC colonies from which the fibroblast-like cells were derived (Figure 1C1-E1). However, hESC-MSCs were positive for the mesenchymal cell markers CD90, CD73 and CD105 (Supplemental Figure S2A1-A3).

#### ASSESSMENT OF CARDIOMYGENIC DIFFERENTIATION

##### *Human-specific immunocytological evaluation*

At day 10 of co-culture with nrCMCs,  $7.17 \pm 0.4\%$  eGFP-labeled hESC-MSCs ( $n = 1,500$  cells analyzed from 5 different isolations) were positive for the sarcomeric protein  $\alpha$ -actinin (Figure 2A1 and 2E), which was a significantly higher fraction than the percentage of fetal hMSCs staining for  $\alpha$ -actinin (fetal amniotic MSCs  $2.15 \pm 0.2\%$ , fetal BM MSCs  $1.8 \pm 0.3\%$  and fetal UC MSCs  $2.56 \pm 0.7\%$ ,  $n = 1,200$  cells analyzed from 4 different isolations per type of fetal hMSC) ( $P < 0.001$ ) (Figure 2B and 2E). Furthermore, in some of the hESC-MSCs (30.8%), fetal amniotic MSCs (25.8%) and fetal BM MSCs (5.89%)  $\alpha$ -actinin was distributed in a cross-striated pattern typical for CMCs. After 10 days of co-culture with nrCMCs, adult BM and adipose MSCs did not stain for  $\alpha$ -actinin ( $n = 1,200$  cells analyzed from 4 different isolations per type of adult hMSC) (Figure 2C and 2E). eGFP-labeled fetal hSFBs in co-culture with nrCMCs were not positive for  $\alpha$ -actinin ( $n = 1,200$  cells analyzed from 4 different isolations) (Figure 2D and 2E) indicating that not all fibroblastic human cell types acquire cardiomyocyte properties in co-culture with nrCMCs. To exclude fusion of nrCMCs with hMSCs or secondary transduction of nrCMCs with eGFP, all co-cultures were also stained for human-specific lamin A/C. None of the eGFP positive cells were negative for human-specific lamin A/C or contained multiple nuclei ( $n \geq 8,500$  eGFP-positive cells analyzed) confirming the validity of the assay system.

To assess the influence of the cellular microenvironment on cardiomyogenic differentiation of hESC-MSCs and fetal hMSCs the presence of  $\alpha$ -actinin in these cells after 10 days of co-culture with nrCFBs rather than nrCMCs was determined. Alpha-actinin was not expressed by hESC-MSCs (Figure 3A1) or any of the fetal hMSC types (Figure 3A2) after co-culture with nrCFBs ( $n = 1,200$  cells analyzed from 3 different isolation of each hMSC type) (Figure 3B).

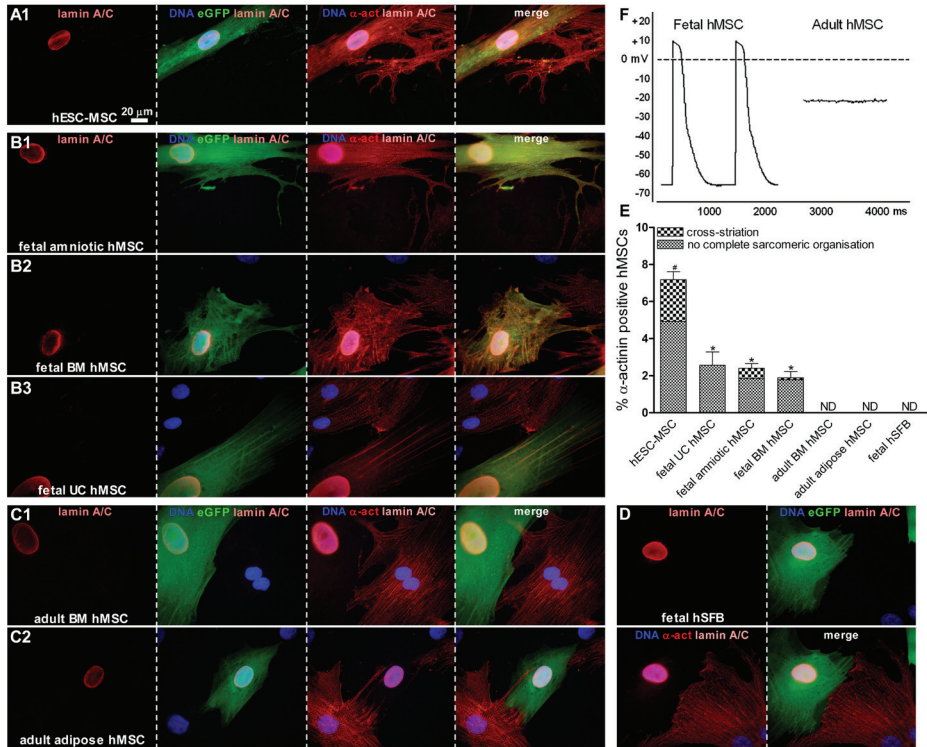


**Figure 2.** Immunocytological assessment of cardiomyogenic differentiation of different types of hMSCs after 10 days of co-culture with nrCMCs. (A1-B3) A fraction of eGFP-labeled, human-specific lamin A/C positive hESC-MSCs and fetal amniotic, BM and UC hMSCs expressed  $\alpha$ -actinin (indicated as  $\alpha$ -act), while (C1-C2) adult BM and adipose hMSCs did not. (D) eGFP-labeled human fetal skin fibroblasts (hSFBs; negative control cells) in co-culture with nrCMCs did not stain positive for  $\alpha$ -actinin. (E) Quantitative analysis of the cardiomyogenic differentiation of different types of hMSCs. The graph is based on a minimum of 1,200 cells analyzed from 4 separate isolations per hMSC type.  $^{\#}P < 0.001$  vs all fetal and adult hMSC types;  $^{*}P < 0.05$  vs adult hMSCs; ND is not detected. (F) Intracellular electrophysiological measurements in fetal (amniotic) and adult (adipose) hMSCs at day 10 of co-culture with nrCMCs and after pharmacological uncoupling of gap junctions. Intrinsic action potentials could be recorded from eGFP-labeled fetal cells, while adult hMSCs showed only steady membrane potentials.

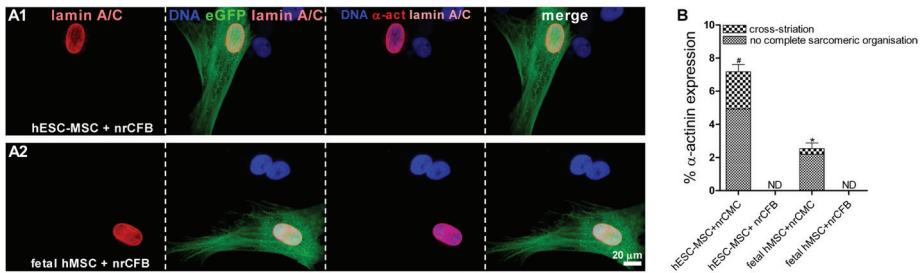


**Figure 3.** Study of cardiomyogenic differentiation in hESC-MSCs and fetal hMSCs after co-culture with nrCFBs for 10 days assessed by immunocytological analysis. (A1-A2) No  $\alpha$ -actinin expression, indicated as  $\alpha$ -act, was detected in eGFP-labeled, human-specific lamin A/C positive hESC-MSCs or fetal hMSCs after co-incubation with nrCFBs. Nuclei were detected with Hoechst. (B) Quantitative analysis of cardiomyogenic differentiation of hESC-MSCs and all of the fetal hMSC types co-cultured with nrCFBs or nrCMCs. The graph is based on a minimum of 1,200 cells analyzed from 3 separate isolations per hMSC type.  $^{\#}P < 0.001$  vs hESC-MSCs and fetal hMSCs co-cultured with nrCFBs and fetal hMSCs in co-culture with nrCMCs;  $^{*}P < 0.01$  vs fetal hESC-MSCs and fetal hMSCs co-cultured with nrCFBs; ND is not detected.

#### *Intracellular electrophysiological measurements in pharmacologically uncoupled hMSCs in co-culture with nrCMCs.*

Patch-clamp recordings were obtained from eGFP-labeled fetal and adult hMSCs at day 10 of co-culture with nrCMCs after electrical isolation through incubation with the gap junction uncoupler 2-APB. Action potentials could only be measured in fetal hMSCs ( $n=5$ , amniotic), this in contrast to adult hMSCs ( $n=8$ , adipose), which only showed steady membrane potentials (Figure 2F). Selection of cells was based on eGFP-labeling and the presence of 2-4 nrCMCs adjacent to the cells of interest.

#### *Human-specific qRT-PCR analysis to detect pluripotency and cardiac differentiation*

qRT-PCR showed that at the mRNA level, hESC-MSCs expressed the following cardiac markers: *Nkx2.5*, *GATA-4*, *ANP*, *MLC2v* and *Cx43*. These mRNAs were upregulated after co-culture with nrCMCs ( $P < 0.001$  for both *ANP* and *MLC2v*;  $P < 0.01$  for *Nkx2.5*;  $P < 0.05$  for both *GATA-4* and *Cx43*). However, *Islet-1* and *c-kit* mRNA levels were lower in co-cultured hESC-MSCs compared to hESC-MSC monocultures ( $P < 0.01$  and  $P < 0.05$ , respectively). No significant difference in gene expression of *VEGF* was detected in hESC-MSCs before or after co-incubation with nrCMCs (Figure 4A). Fetal amniotic hMSCs showed an increase in *Nkx2.5* ( $P < 0.05$ ), *ANP*, *Cx43* and *VEGF* (all  $P < 0.01$ ) gene expression after co-culture with nrCMCs, while *Islet-1* mRNA levels were decreased under these circumstances ( $P < 0.05$ ). No

difference in *c-kit* gene expression was detected in these fetal hMSCs before or after co-incubation with nrCMCs (Figure 4B). In fetal UC hMSCs, mRNA levels of *GATA-4*, *Cx43* (both  $P < 0.05$ ) and *VEGF* ( $P < 0.001$ ) were significantly upregulated after their co-culture with nrCMCs, while *Islet-1* and *c-kit* gene expression were downregulated ( $P < 0.001$  and  $P < 0.01$ , respectively). No change in the expression of *ANP* was detected in fetal UC hMSCs following co-incubation with nrCMCs (Figure 4C). Fetal BM hMSCs showed an increase in *ANP* ( $P < 0.001$ ), *Cx43* and *c-kit* (both  $P < 0.05$ ) gene expression co-incubation with nrCMCs, while no difference in *Islet-1* and *VEGF* mRNA levels were detected under these circumstances (Figure 4D). At the mRNA level, *ANP*, *Cx43*, *VEGF* and *c-kit* were detected in adult BM and adipose hMSCs. However, after co-culture with nrCMCs, only the expression of *ANP* ( $P < 0.05$ ) and *VEGF* ( $P < 0.01$ ) increased in both types of adult hMSCs. In adult adipose hMSCs *c-kit* mRNA levels were also upregulated in the presence of nrCMCs ( $P < 0.05$ ) (Figure 4E-4F). *Oct-4*, *Nanog*, *cTnI* and  $\beta$ -*MHC* gene expression was not detected in any of the hMSC types. qRT-PCR analysis of RNA from appropriate human control samples confirmed the functionality of all human-specific primer pairs. The same primer pairs did not give rise to amplification products using nrCMC RNA as starting material. Expression of the qRT-PCR target genes in nrCMCs was confirmed using rat-specific primers. Quantitative differences in gene expression between hMSCs cultured alone or with nrCMCs are given in supplemental table S2.

*Optical mapping analysis to determine action potential CV in co-cultures of nrCMCs with different types of hMSCs*

CV in nrCMC co-cultures with hESC-MSCs ( $25.9 \pm 0.9$  cm/s) was similar to the CV in nrCMC cultures alone ( $24.8 \pm 1.2$  cm/s) (Figure 5B1-B2 and 5C). However, it was significantly higher than in co-cultures of nrCMCs with fetal amniotic hMSCs ( $22.0 \pm 1.8$  cm/s), adult adipose hMSCs ( $18.2 \pm 1.1$  cm/s) and nrCFBs ( $17.0 \pm 1.2$  cm/s) ( $P < 0.001$ ;  $n \geq 15$  co-cultures with each cell type) (Figure 5B3-B5 and C). CV was also higher in co-cultures of nrCMCs with fetal amniotic hMSCs than in co-cultures with adult adipose hMSCs or with nrCFBs ( $P < 0.001$ ) (Figure 5B3-B5 and C).

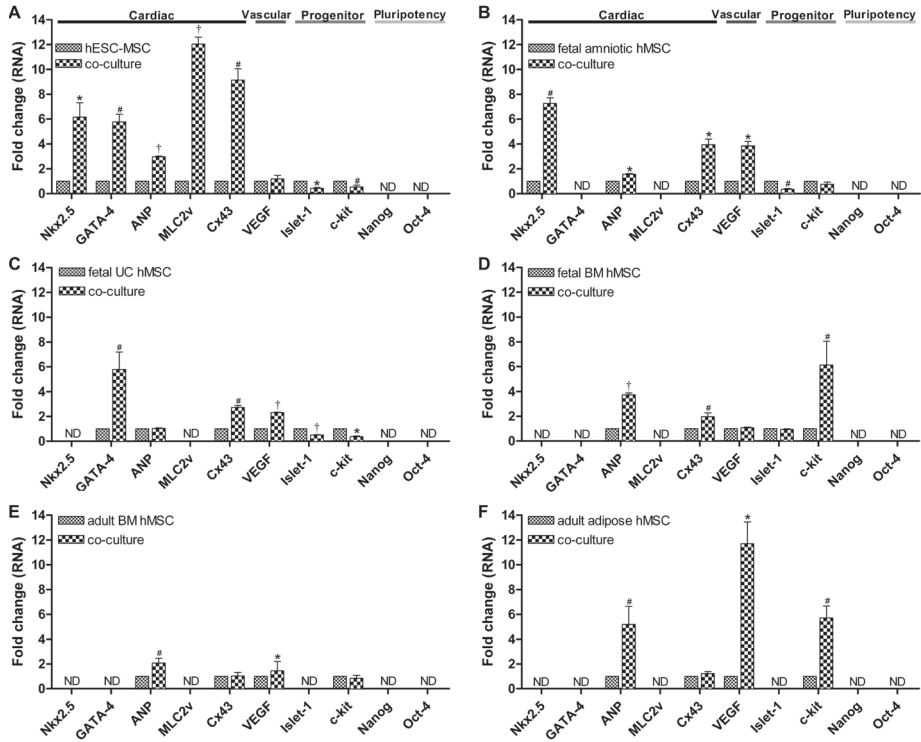


**Figure 4.** Analysis by qRT-PCR of expression of pluripotency and cardiac genes in hMSCs alone or after co-incubation with nrCMCs. (A) hESC-MSCs expressed most cardiac-specific genes, which were significantly upregulated after co-incubation with nrCMCs. Expression of the cardiac progenitor genes, *Islet-1* and *c-kit*, was downregulated in the presence of nrCMCs. (B-D) The fetal hMSC types expressed a variety of cardiac-specific genes, which were upregulated after co-culture with nrCMCs. *Islet-1* and *c-kit* mRNA levels decreased in the presence of nrCMCs with the exception of the upregulation of *c-kit* gene expression in fetal BM MSCs following their co-culture with nrCMCs. (E-F) *ANP*, *Cx43*, *VEGF* and *c-kit* gene expression was detected in adult hMSCs before and after co-incubation with nrCMCs. (A-F) hMSCs did not express the pluripotency genes *Oct-4* and *Nanog*. # $P < 0.05$  vs specific hMSC monoculture; \* $P < 0.01$  vs specific hMSC monoculture; † $P < 0.001$  vs specific hMSC monoculture.

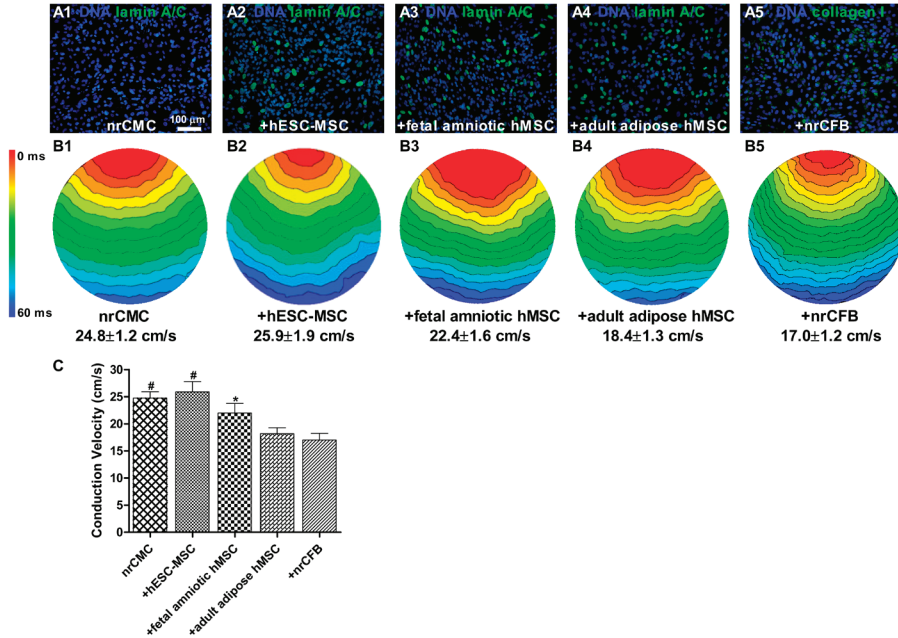


**Figure 5.** Assessment of CV by optical mapping in co-cultures of nrCMCs and different types of hMSCs. (A) The presence of hMSCs and nrCFBs after optical mapping was confirmed by immunostaining for human-specific lamin A/C and collagen type I, respectively. Nuclei were detected with Hoechst. (B) Activation maps of the different (co-)cultures reveal significantly higher CVs in nrCMCs monocultures and in hESC-MSCs/nrCMC and fetal amniotic hMSCs/nrCMC co-cultures than in co-cultures of nrCMCs with adult adipose hMSCs or with nrCFBs. CVs were also significantly higher in nrCMC monocultures and in hESC-MSCs/nrCMC co-cultures than in co-cultures between nrCMCs and fetal amniotic hMSCs. Spacing of isochronal lines in activation maps is 4 ms, and colors indicate temporal sequence of activation, starting from the red area. (C) Bar graph of the CVs in nrCMC monocultures and in co-cultures (+) between nrCMCs and nrCFBs or different types of hMSCs as indicated. # $P < 0.001$  vs fetal amniotic hMSCs, adult adipose hMSCs and nrCFBs co-incubated with nrCMCs; \* $P < 0.01$  vs adult adipose hMSCs and nrCFBs co-incubated with nrCMCs.

**IN VITRO ANGIOGENESIS ASSAYS**

hESC-MSCs and all types of fetal hMSCs were able to form capillary-like structures on Matrigel ( $n \geq 5$  isolations of each hMSC type incubated in triplicate) (Figure 6A1-D1). These networks stained positively for the smooth muscle marker smMHC and the endothelial cell marker PECAM-1 (Figure 6A2-D2). Formation of cellular networks was established by hESC-MSCs 12 h after incubation on Matrigel. For hMSCs derived from the fetal sources it took 18 h to establish capillary-like networks. Adult BM and adipose tissue hMSCs failed to form capillary-like structures ( $n \geq 5$  isolations of each hMSC type incubated in triplicate) (Figure 6E-F). Formation of vessel-like networks was checked every hour for a total period of 24 h.

**EVALUATION OF CX43 EXPRESSION LEVELS**

To further analyze mechanisms underlying differences in cardiomyogenic potential, Cx43 expression levels were evaluated. Immunocytological analysis showed that Cx43 protein expression was more abundant in hESC-MSCs and fetal amniotic MSCs than in adult adipose MSCs and nrCFBs ( $n = 5$  isolations of each hMSC type were assessed) (Figure 7A). These results were confirmed by Western blot analysis ( $n = 5$  different isolations for each cell type) (Figure 7C). Cx43 expression was also detected at the interfaces between nrCMCs and hESC-MSCs or fetal MSCs, while under equivalent staining conditions it was not present at contact-areas between nrCMCs and adult hMSCs or nrCFBs (Figure 7A). Moreover, Cx43 did not line borders between nrCFBs and any of the types of hMSCs ( $n \geq 1,500$  cells analyzed from 5 isolations of each cell type under each condition) (Figure 7A). qRT-PCR showed a significant increase in Cx43 expression following the incubation of hESC-MSCs or fetal amniotic hMSCs with nrCMCs ( $9.14 \pm 0.9$  ( $P < 0.01$ ) and  $3.94 \pm 0.5$  fold ( $P < 0.001$ ), respectively), while no (hESC-MSCs) or  $19.4 \pm 0.1$  fold less (fetal amniotic hMSCs) Cx43 mRNA was detected in co-cultures with nrCFBs ( $P < 0.05$ ) (Figure 7B1-B2). No significant difference in Cx43 mRNA levels was detected between adult adipose tissue hMSCs cultured alone or together with nrCMCs or nrCFBs (Figure 7B3).

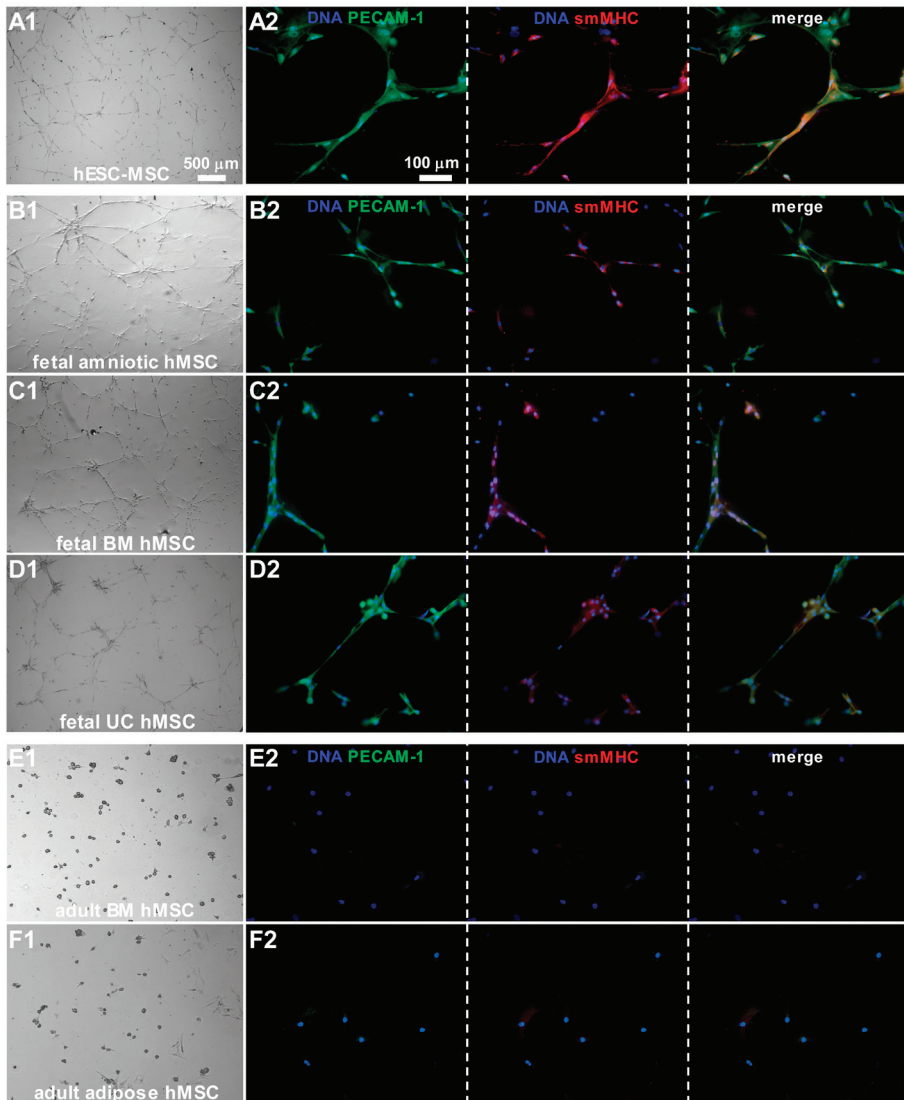


**Figure 6.** Angiogenic differentiation capacity of different types of hMSCs assessed by formation of capillary-like structures and expression of angiogenic markers following their culture on Matrigel. (A1-D1) Bright field images show that hESC-MSCs and fetal hMSCs were able to form stable cellular networks on a basement membrane matrix, while (E1-F1) adult hMSCs could not. (A2-D2) hESC-MSCs and all fetal hMSC types stained positive for the endothelial cell protein, PECAM-1, and the smooth muscle cell protein, smMHC, while (E2-F2) the adult hMSCs were negative for these markers. Nuclei were stained with Hoechst.

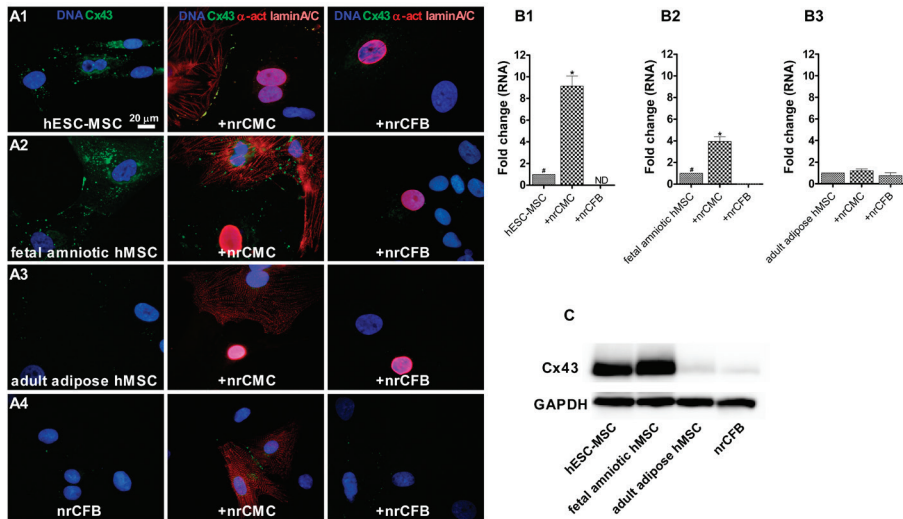


**Figure 7.** Analysis by immunofluorescence microscopy, qRT-PCR and Western blotting of Cx43 expression in hMSC monocoltures and in co-cultures of nrCMCs or nrCFBs with different types of hMSCs. (A1-A2) Immunocytological analysis shows high Cx43 levels in monocoltures of hESC-MSCs and fetal amniotic hMSCs. Cx43 was also detected at the interfaces of these young hMSCs with nrCMCs but not with nrCFBs. nrCMCs were visualized by staining with  $\alpha$ -actinin (indicated as  $\alpha$ -act), while an antibody against human-specific lamin A/C was used to detect hMSCs. Nuclei were detected with Hoechst. (A3-A4) Adult adipose hMSCs contain very low amounts of Cx43 in both monocoltures and co-cultures with nrCMCs or nrCFBs. Also in nrCFB monocoltures and nrCFB/nrCMC co-cultures Cx43 is barely detectable. (B1-B3) Bar graphs of the assessment by qRT-PCR of Cx43 mRNA levels in hESC-MSC, fetal amniotic hMSC and adult adipose hMSC monocoltures and co-cultures (+) of these cells with either nrCMCs or nrCFBs as indicated. (C) Picture of representative part of a Western blot showing that hESC-MSCs and fetal amniotic hMSCs contain large amounts of Cx43 in contrast to adult adipose hMSCs and nrCFBs. The housekeeping protein glyceraldehyde-3-phosphate dehydrogenase (GAPDH) was used to check for equal protein loading. # $P < 0.05$  vs hMSCs in co-culture with nrCFBs; \* $P < 0.01$  vs hMSC monocoltures and hMSCs in co-culture with nrCFBs.

## DISCUSSION

Key findings of the present study are: 1) Differentiation potential of hMSCs toward three cardiac cell lineages depends on the developmental stage of donor tissue; 2) Cardiomyogenesis of hMSCs is influenced by stimuli from the cellular microenvironment; and 3) The propensity of different types of hMSCs to acquire properties of heart muscle cells correlates with Cx43 expression levels.

### DEVELOPMENT AND STEMNESS

During embryonic development, stem cells contribute to organ formation, while later in life these cells or their derivatives are involved in repair and regeneration of organs [6]. However, with increasing age, the potential of stem cells declines [19,20]. This decrease in the regenerative ability is associated with cumulative organ dysfunction, which may lead to increased morbidity and mortality. Consistent with this developmental stage-dependent decline in function of stem cells, this study showed that MSCs derived from hESCs have significantly greater proliferative capacity and longer telomeres than MSCs derived from human fetal tissue, or adult hMSCs. The intrinsic age-associated decrease in telomere length is one of the mechanisms that contributes to the loss of stem cell properties with age [21]. The results of this first-time direct comparison of the proliferative capacity of hESC-MSCs, fetal hMSCs and adult hMSCs are in line with previous studies [12,13,22–24]. All together, these findings show that MSCs derived from human ESCs are more immature and display greater stemness than those derived from fetal tissues.

### MSCS AND CARDIAC DIFFERENTIATION

In the present study, it was also shown that hMSCs derived from either embryonic or fetal sources have the capacity to undergo cardiac differentiation, while those derived from adult sources do not. Our results revealed that developmental stage of the donor tissue not only influences the ability of hMSCs to differentiate into CMCs but also their capacity to undergo smooth muscle and endothelial differentiation. This information may be of value in extending the repertoire of cells considered suitable for studies of cardiac repair. We showed that after co-culture with nrCMCs the sarcomeric protein  $\alpha$ -actinin is expressed by a significantly higher percentage of hESC-MSCs than of fetal hMSCs, while it was not expressed by adult hMSCs. Although the cardiomyogenic potential of MSCs derived from neonatal sources has been described before, a direct comparison of hMSCs derived from embryonic, fetal and adult sources was not conducted [9,10]. Controversy still exists on whether MSCs actually differentiate into CMCs or whether this apparent cardiomyogenesis is due to fusion of MSCs with CMCs [25]. Therefore, in all our co-culture experiments eGFP-transduced hMSCs were stained for human-specific

lamin A/C. Neither multinucleated eGFP positive cells nor eGFP positive cells negative for human-specific lamin A/C were detected. In addition, only human-specific primers were used in the qRT-PCR experiments to exclude detection of rat cardiac-specific genes expressed by nrCMCs. Accordingly, the cardiomyogenic differentiation of hMSCs observed in our experiments does not result from cell fusion. Importantly, the records of intrinsic action potentials in eGFP positive cells at day 10 of co-culture provides direct evidence for functional cardiomyogenic differentiation.

With respect to smooth muscle and endothelial differentiation, only hESC-MSCs and fetal hMSCs were able to form capillary-like structures on Matrigel. These networks stained positive for the smooth muscle marker smMHC and the endothelial marker PECAM-1. Previous studies showed that adult BM-derived MSCs were able to form capillary-like structures after priming the cells in endothelial differentiation medium. However, after priming, UC hMSCs had higher endothelial potential than adult BM hMSCs [26,27].

Concerning the underlying mechanisms why adult hMSCs do not form CMCs, Cx43 expression may be of importance. In this study, hMSCs are co-cultured with nrCMCs, resulting in physical contact between these two cell types, and allowing the possibility for gap junction formation. Gap junctions, which in the ventricles are mainly formed by Cx43, allow a low-resistant spread of chemical and electrical signals between adjacent cells [28]. Interestingly, hMSCs derived from adult human sources express very low levels of Cx43, both at mRNA and protein level, as compared to hMSCs derived from embryonic and fetal sources. In addition, hMSCs, which underwent functional cardiomyogenic differentiation, were always adjacent to native CMCs, naturally containing high levels of Cx43. As hMSCs are able to form functional gap junctions with adjacent CMCs [29], electrical and chemical interaction can occur between both cell types and this was shown to play a role in cardiomyogenic differentiation [30]. Interestingly, co-culture of MSCs with cardiac fibroblasts, expressing very low levels of Cx43, did not result in cardiomyogenic differentiation. In fact, using human-specific primers, Cx43 expression levels in hMSCs were shown to decrease significantly in this microenvironment.

As Cx43 plays an essential role in myocardial electrical conduction across the ventricular muscle, and cardiomyogenic differentiation would make non-excitable MSCs become excitable, we also studied the CV across co-cultures of hMSCs with nrCMCs. It was shown that co-cultures with hESC-MSCs showed a significantly higher CV than those with fetal hMSCs and adult hMSCs, while the CV in co-cultures with fetal hMSCs was also significantly higher than that in those with adult hMSCs. Of note, embryonic MSCs did not only show high expression of Cx43, but had the greatest cardiomyogenic differentiation potential. The type of MSC that

contributes to the highest CV may be preferable to accomplish functional integration with host myocardium after transplantation.

#### **MSC TRANSPLANTATION FOR CARDIAC DISEASES**

Besides providing new insights into the factors that stimulate cardiac differentiation, the findings of this study may also have implications for the use of MSCs in patients. Currently, in myocardial cell therapy studies mainly autologous cells from aged patients suffering from chronic diseases are used. Based on our results, it may be expected that the therapeutic effects of MSC transplantation, to improve cardiac function, are affected by intrinsic properties of the transplanted cells. Furthermore, the beneficial effects of stem cell therapy in the damaged heart seems to be largely mediated by paracrine factors promoting neo-angiogenesis and CMC survival with little evidence of the differentiation of transplanted cells into CMCs [3]. As these effects will be of limited help in case of extensive loss of myocardial tissue there is still a great demand for stem cells that can differentiate *in vivo* into new CMCs. In this study, we have shown that hMSCs of prenatal origin can differentiate into functional CMCs and that this process is dependent on instructive cues provided by neighboring CMCs. Therefore selection of MSCs from donor sources, such as the umbilical cord or amniotic membrane/fluid, may be an attractive source of immature or young cells for autologous cell transplantation. Even allogeneic transplantation may be considered as MSCs are reported to have immunomodulatory properties [31–33]. However, many aspects related to transplantation of cardiomyogenic stem cells need to be studied in more detail before optimal therapeutic efficacy and minimal hazardous potential can be achieved.

#### **CONCLUSIONS**

Human MSCs of embryonic stem cell or fetal but not adult origin can differentiate into three cardiac lineages: cardiomyocytes, endothelial cells and smooth muscle cells. The ability to undergo functional cardiomyogenic differentiation is amongst others determined by the microenvironment of the cells, in particular their communication with adjacent cell types. The gap junction protein Cx43 may play an important role in this differentiation process.

#### **STUDY LIMITATIONS**

It would have been more clinically relevant to co-culture the different hMSC subtypes with adult human hCMCs, but obtaining these cells in the numbers needed to conduct these experiments seems not feasible. Furthermore, adult hCMCs cannot be cultured long enough to perform some of the key experiments described in this paper.

## ACKNOWLEDGEMENTS

The technicians of the stem cell laboratory of the LUMC are gratefully acknowledged for expansion of adult BM hMSCs.

## REFERENCES

1. Lloyd-Jones D, Adams R, Carnethon M, De SG, Ferguson TB et al. (2009) Heart disease and stroke statistics--2009 update: a report from the American Heart Association Statistics Committee and Stroke Statistics Subcommittee. *Circulation* 119: 480-486.
2. Ballard VL, Edelberg JM (2007) Stem cells and the regeneration of the aging cardiovascular system. *Circ Res* 100: 1116-1127.
3. Passier R, van Laake LW, Mummery CL (2008) Stem-cell-based therapy and lessons from the heart. *Nature* 453: 322-329.
4. O'Donoghue K, Fisk NM (2004) Fetal stem cells. *Best Pract Res Clin Obstet Gynaecol* 18: 853-875.
5. Roobrouck VD, Ulloa-Montoya F, Verfaillie CM (2008) Self-renewal and differentiation capacity of young and aged stem cells. *Exp Cell Res* 314: 1937-1944.
6. Ballard VL (2010) Stem cells for heart failure in the aging heart. *Heart Fail Rev* 15: 447-56.
7. Semenov OV, Koestenbauer S, Riegel M, Zech N, Zimmermann R et al. (2010) Multipotent mesenchymal stem cells from human placenta: critical parameters for isolation and maintenance of stemness after isolation. *Am J Obstet Gynecol* 202: 193.
8. Jo CH, Kim OS, Park EY, Kim BJ, Lee JH et al. (2008) Fetal mesenchymal stem cells derived from human umbilical cord sustain primitive characteristics during extensive expansion. *Cell Tissue Res* 334: 423-433.
9. Nishiyama N, Miyoshi S, Hida N, Uyama T, Okamoto K et al. (2007) The significant cardiomyogenic potential of human umbilical cord blood-derived mesenchymal stem cells in vitro. *Stem Cells* 25: 2017-2024.
10. Pijnappels DA, Schaliij MJ, Ramkisoensing AA, van Tuyn J, de Vries AA et al. (2008) Forced alignment of mesenchymal stem cells undergoing cardiomyogenic differentiation affects functional integration with cardiomyocyte cultures. *Circ Res* 103: 167-176.
11. Hwang NS, Varghese S, Lee HJ, Zhang Z, Ye Z et al. (2008) In vivo commitment and functional tissue regeneration using human embryonic stem cell-derived mesenchymal cells. *Proc Natl Acad Sci U S A* 105: 20641-20646.
12. Lian Q, Lye E, Suan YK, Khia Way TE, Salto-Tellez M et al. (2007) Derivation of clinically compliant MSCs from CD105+. *Stem Cells* 25: 425-436.
13. Olivier EN, Rybicki AC, Bouhassira EE (2006) Differentiation of human embryonic stem cells into bipotent mesenchymal stem cells. *Stem Cells* 24: 1914-1922.
14. Trivedi P, Hematti P (2008) Derivation and immunological characterization of mesenchymal stromal cells from human embryonic stem cells. *Exp Hematol* 36: 350-359.
15. Barberi T, Willis LM, Socci ND, Studer L (2005) Derivation of multipotent mesenchymal precursors from human embryonic stem cells. *PLoS Med* 2: e161.
16. Karlsson C, Emanuelsson K, Wessberg F, Kajic K, Axell MZ et al. (2009) Human embryonic stem cell-derived mesenchymal progenitors-Potential in regenerative medicine. *Stem Cell Res* 3:39-50.

- 44
17. Bai D, del CC, Srinivas M, Spray DC (2006) Block of specific gap junction channel subtypes by 2-aminoethoxydiphenyl borate (2-APB). *J Pharmacol Exp Ther* 319: 1452-1458.
  18. Harks EG, Camina JP, Peters PH, Ypey DL, Scheenen WJ et al. (2003) Besides affecting intracellular calcium signaling, 2-APB reversibly blocks gap junctional coupling in confluent monolayers, thereby allowing measurement of single-cell membrane currents in undissociated cells. *FASEB J* 17: 941-943.
  19. Bellantuono I, Keith WN (2007) Stem cell ageing: does it happen and can we intervene? *Expert Rev Mol Med* 9: 1-20.
  20. Chambers SM, Goodell MA (2007) Hematopoietic stem cell aging: wrinkles in stem cell potential. *Stem Cell Rev* 3: 201-211.
  21. Torella D, Rota M, Nurzynska D, Musso E, Monsen A et al. (2004) Cardiac stem cell and myocyte aging, heart failure, and insulin-like growth factor-1 overexpression. *Circ Res* 94: 514-524.
  22. In 't Anker PS, Scherjon SA, Kleijburg-van der KC, de Groot-Swings GM, Claas FH et al. (2004) Isolation of mesenchymal stem cells of fetal or maternal origin from human placenta. *Stem Cells* 22: 1338-1345.
  23. Roubelakis MG, Pappa KI, Bitsika V, Zagoura D, Vlahou A et al. (2007) Molecular and proteomic characterization of human mesenchymal stem cells derived from amniotic fluid: comparison to bone marrow mesenchymal stem cells. *Stem Cells Dev* 16: 931-952.
  24. Miao Z, Jin J, Chen L, Zhu J, Huang W et al. (2006) Isolation of mesenchymal stem cells from human placenta: comparison with human bone marrow mesenchymal stem cells. *Cell Biol Int* 30: 681-687.
  25. Alvarez-Dolado M (2007) Cell fusion: biological perspectives and potential for regenerative medicine. *Front Biosci* 12: 1-12.
  26. Oswald J, Boxberger S, Jorgensen B, Feldmann S, Ehninger G et al. (2004) Mesenchymal stem cells can be differentiated into endothelial cells in vitro. *Stem Cells* 22: 377-384.
  27. Chen MY, Lie PC, Li ZL, Wei X (2009) Endothelial differentiation of Wharton's jelly-derived mesenchymal stem cells in comparison with bone marrow-derived mesenchymal stem cells. *Exp Hematol* 37: 629-640.
  28. Kleber AG, Rudy Y (2004) Basic mechanisms of cardiac impulse propagation and associated arrhythmias. *Physiol Rev* 84: 431-488.
  29. Pijnappels DA, Schalijs MJ, van Tuyn J, Ypey DL, de Vries AA et al. (2006) Progressive increase in conduction velocity across human mesenchymal stem cells is mediated by enhanced electrical coupling. *Cardiovasc Res* 72: 282-291.
  30. van Vliet P, de Boer TP, van der Heyden MA, El Tamer MK, Sluijter JP et al. (2010) Hyperpolarization Induces Differentiation in Human Cardiomyocyte Progenitor Cells. *Stem Cell Rev* 6:178-85.
  31. Yoo KH, Jang IK, Lee MW, Kim HE, Yang MS et al. (2009) Comparison of immunomodulatory properties of mesenchymal stem cells derived from adult human tissues. *Cell Immunol* 259: 150-156.
  32. Liechty KW, MacKenzie TC, Shaaban AF, Radu A, Moseley AM et al. (2000) Human mesenchymal stem cells engraft and demonstrate site-specific differentiation after in utero transplantation in sheep. *Nat Med* 6: 1282-1286.
  33. Hare JM, Traverse JH, Henry TD, Dib N, Strumpf RK et al. (2009) A randomized, double-blind, placebo-controlled, dose-escalation study of intravenous adult human mesenchymal stem cells (prochymal) after acute myocardial infarction. *J Am Coll Cardiol* 54: 2277-2286.

## SUPPLEMENTAL MATERIALS AND METHODS S1

### EXPANDED MATERIALS & METHODS

#### ISOLATION AND CULTURE OF HUMAN MESENCHYMAL STEM CELLS (hMSCs)

All human-derived tissues were collected based on individual written (parental) informed consent, after approval by the Medical Ethics committee of the Leiden University Medical Center (LUMC), where all investigations were performed. The investigation conforms with the principles outlined in the Declaration of Helsinki.

#### *Derivation of MSCs from human embryonic stem cells (hESCs)*

MSCs were derived from undifferentiated hESC colonies (hES3 subclones) as previously described [1,2]. Briefly, the undifferentiated hESC colonies were removed from their mouse embryonic fibroblast (mEF) feeder layer and propagated in gelatin-coated culture dishes in standard MSC culture medium (Dulbecco's modified Eagle's medium [Invitrogen, Breda, The Netherlands] containing 10% fetal bovine serum [FBS; Invitrogen], penicillin [100 U/mL] and streptomycin [100 µg/mL]; hereinafter referred to as MSC-CM) at 37°C in a humidified 5% CO<sub>2</sub> incubator. After 2-3 days of culture, a portion of the cells at the periphery of the hESC colonies differentiated toward spindle-shaped fibroblast-like cells. Next, the undifferentiated portions of the hESC colonies were removed by physical scraping and suctioning. Consecutive enzymatic passaging as single cell suspensions led to a reproducible derivation of morphologically homogeneous fibroblast-like cells from cultures of pluripotent undifferentiated hESCs within 2-3 passages (n=5 different isolations). Medium was replaced twice a week until the primary cultures were 60-80% confluent, after which the so-called hESC-MSCs were amplified by serial passage using a buffered 0.05% trypsin-0.02% ethylenediaminetetraacetic acid/EDTA solution (TE; BioWhittaker, Vervier, Belgium) for cell detachment.

#### *Fetal hMSC isolation and culture*

Human fetal tissues (gestational age between 17-22 weeks) were collected through legal interventions by the Department of Obstetrics. Fetal umbilical cords (UCs) and amniotic membranes were washed twice with phosphate-buffered saline (PBS) and were finely minced into 1-2 mm fragments using scissors and scalpels. Cells were released by treatment with 0.1% collagenase type I (Worthington, Lakewood, NJ, USA) for 3 h. Thereafter, 10 mL MSC-CM was added. The cell suspension was transferred to a 25-cm<sup>2</sup> culture flask (Becton Dickinson, Franklin Lakes, NJ, USA) and incubated for 3-4 days at 37°C in a humidified 5% CO<sub>2</sub> atmosphere to allow the cells to adhere. Fetal UC and amniotic membrane (amniotic) hMSCs were subcultured as described in the previous section. Single cell suspensions of fetal bone

marrow (BM) were obtained by punching fetal *femora* and *tibiae* with a 23-gauge needle and flushing them with culture medium. The cell suspension was centrifuged at 330 g for 10 min after which the same culture methods were applied as for the other fetal hMSCs. To obtain human fibroblasts, sections of human fetal skin (5×5 mm) were transferred to 25-cm<sup>2</sup> culture flasks containing 5 ml MSC-CM and maintained in a humidified 5% CO<sub>2</sub> incubator at 37°C. Fetal human skin fibroblasts (hSFBs) were allowed to migrate from the skin sections for 7 days. Thereafter, the skin sections were removed and the remaining hSFBs were cultured using standard procedures.

#### *Adult MSC isolation and culture*

Adult hMSCs were purified from leftover BM samples derived from adult donors undergoing orthopedic surgery (n=8 donors, mean donor age 72±2.4 yrs). Briefly, the mononuclear cell fraction of the BM was isolated by Ficoll density gradient centrifugation. Twenty-four hours after seeding of the BM mononuclear cell fraction in 75-cm<sup>2</sup> culture flasks (Becton Dickinson), the non-adherent cells were removed and the remaining hMSCs were expanded by serial passage using standard methods.

Adult adipose tissue (adipose) hMSCs were derived from subcutaneous abdominal fat tissue (n= 10 donors, mean donor age 39.6±1.1 yrs). Tissue samples were washed twice with PBS containing penicillin (100 U/mL) and streptomycin (100 µg/mL). For tissue disruption 0.1% collagenase type I solution was added and tissue samples were finely minced. Next, samples were incubated at 37°C in a humidified 5% CO<sub>2</sub> incubator for 1 h. Collagenase type I activity was quenched by adding excess MSC-CM. Samples were then centrifuged at 330 g for 10 min. After centrifugation the layer of primary adipocytes could be removed and the collagenase type I-containing solution was aspirated. The cell pellet was resuspended in MSC-CM, filtered through a 70 mm cell strainer (Becton Dickinson) and the cells were once again collected by centrifugation. This step was repeated twice, after which the cell pellet was resuspended in 5 ml culture medium. The resulting cell suspension was transferred to a 25-cm<sup>2</sup> culture flask and these adult adipose tissue (adipose) hMSCs were propagated as all the other hMSCs.

#### **ISOLATION AND CULTURE OF NEONATAL RAT (NR) CARDIOMYOCYTES (CMCS) AND CARDIAC FIBROBLASTS (CFBS)**

All animal experiments were approved by the Animal Experiments Committee of the LUMC and conform to the Guide for the Care and Use of Laboratory Animals, as stated by the US National Institutes of Health (permit numbers: 09012 and 10236) [3].

nrCMCs and nrCFBs were dissociated from ventricles of 2-day old male Wistar rats, separated from each other by differential plating and maintained in nrCMC

culture medium containing 5% horse serum (Invitrogen), penicillin (100 U/mL; Bio-Whittaker) and streptomycin (100 µg/mL; BioWhittaker), as previously described [4]. nrCFBs were cultured in MSC-CM and passaged at least three times before they were used in co-culture experiments.

Five hundred thousand or one million nrCMCs were plated on collagen type I-coated (Sigma-Aldrich) glass coverslips in 6-well culture dishes and incubated in a humidified incubator at 37 °C and 5% CO<sub>2</sub>. Proliferation of residual nrCFBs in nrCMC cultures was inhibited by incubation of the cells with 100 mmol/L 5-bromo-2-deoxyuridine (Sigma-Aldrich) during the first 24 h after culture initiation.

For optical mapping experiments, 8×10<sup>4</sup> nrCMCs were plated on fibronectin-coated (Sigma-Aldrich) glass coverslips in 24-well culture dishes. As the conduction velocity (CV) through monolayers of nrCMCs is inversely related to their CFB content, prior to their use in co-incubation experiments with hMSCs, the nrCMC cultures were treated for 2 h with 10 mg/mL mitomycin-C (Sigma-Aldrich) to stop proliferation of residual nrCFBs present in these cultures [12].

## CHARACTERIZATION OF hMSCS

### *Flow cytometry*

Analysis of surface marker expression was carried out by flow cytometry. hMSCs (passage<sup>3</sup>) were detached using TE, resuspended in PBS containing 1% bovine serum albumin fraction V (BSA; Sigma-Aldrich) and divided in aliquots of 2×10<sup>5</sup> cells. Cells were then incubated for 30 min at 4°C with fluorescein isothiocyanate-, phycoerythrin- or allophycocyanin-conjugated antibodies directed against human CD105 (Ansell, Bayport, MN, USA), CD90, CD73, CD45, CD34, CD31, CD24 and stage-specific embryonic antigen-4 (SSEA-4) (all from Becton Dickinson). Labeled cells were washed three times with PBS containing 1% BSA and analyzed using an LSR II three-laser, 12-color, flow cytometer (Becton Dickinson). Isotype-matched control antibodies (Becton Dickinson) were used to determine background fluorescence. At least 10<sup>4</sup> cells per sample were acquired and data were processed using FACSDiva software (Becton Dickinson).

### *Adipogenic and osteogenic differentiation of hMSCs*

The hMSCs were characterized by established differentiation assays [5]. Briefly, 5×10<sup>3</sup> hMSCs per well were plated in a 12-well culture plate and exposed to adipogenic or osteogenic differentiation medium. Adipogenic differentiation medium consisted of MEM-plus (i.e. α-minimum essential medium [Invitrogen] containing 15% FBS, 100 U/L penicillin and 100 µg/mL streptomycin) supplemented with insulin, dexamethason, indomethacin and 3-isobutyl-1-methylxanthine (all from Sigma-Aldrich) to final concentrations of 5 µg/mL, 1 µM, 50 µM and 0.5 µM, respectively,

and was refreshed every 3-4 days for a period of 3 weeks. Lipid accumulation was assessed by Oil Red O (Sigma-Aldrich) staining of the cultures (15 mg of Oil Red O/ mL of 60% isopropanol) and light microscopy. Osteogenic differentiation medium consisted of MEM-plus containing 10 mM  $\beta$ -glycerophosphate, 50  $\mu$ g/mL ascorbic acid and 10 nM dexamethason (all from Sigma-Aldrich) and was refreshed every 3-4 days for a period of 3 weeks. Afterwards, the cells were washed with PBS and calcium deposits were visualized by staining of the cells for 5 min with 2% Alizarine Red S (Sigma-Aldrich) in 0.5%  $\text{NH}_4\text{OH}$  (pH 5.5).

#### *Immunocytological characterization of hESC-MSCs*

hESC colonies were originally grown on a feeder layer of mEFs. To verify the human origin of the fibroblast-like cells derived from the hESC colonies, the cells were incubated with a monoclonal antibody (MAb) specific for human lamin A/C (clone 636; Vector laboratories, Burlingame, CA, USA) at a dilution of 1:200, as previously described [6]. Binding of the primary antibody to its target antigen was visualized using Alexa 568-linked donkey anti-mouse IgG secondary antibodies (Invitrogen; dilution 1:200). Murine MSCs (mMSCs) were not labeled with the human lamin A/C-binding MAb, confirming its species specificity.

In addition, hESC-MSCs were stained with antibodies directed against the hESC marker SSEA-4 (MAb MC813; Santa Cruz Biotechnologies, Santa Cruz, CA, USA) or against the pluripotency-associated transcription factors Oct-3/4 (MAb N-19; Santa Cruz) and Nanog (goat polyclonal antibody [PAb]; R&D Systems, Minneapolis, MN, USA). Each of these primary antibodies was applied at a dilution of 1:100. As secondary antibodies we used Alexa 568-conjugated donkey anti-mouse IgG or donkey anti-goat IgG (both from Invitrogen) at a dilution of 1:200. hESC colonies from which the hESC-MSCs were derived, were used as a positive control in these stainings. Lastly, hESC-MSCs were stained with fluorescein isothiocyanate- and phycoerythrin- conjugated antibodies directed against the mesenchymal stem cell markers CD90, CD73 and CD105 at a dilution of 1:200.

#### *Growth kinetics*

Growth kinetics of the hMSCs was analyzed by calculating population doublings (PDs). Each type of hMSC was plated in triplicate at a concentration of  $2 \times 10^3$  hMSCs per  $\text{cm}^2$  in 25- $\text{cm}^2$  culture flasks ( $n=3$  isolations for each type of hMSC). After every 5 days of culture at 37°C in 95% humidified air-5%  $\text{CO}_2$ , the cells were trypsinized and resuspended in 5 mL. Subsequently, a part of each cell suspension was subjected to Trypan Blue staining to determine the viable cell concentration using a hemocytometer. This information was used to initiate the next cell passage in a new culture flask and to determine the number of PDs during the previous culture period.

*Relative telomere length using quantitative real-time polymerase chain reaction (qRT-PCR)*

Genomic DNA from experimental ( $n^36$  samples of ESC-derived, fetal or adult MSCs cultured for the same period of time) and reference samples was obtained using DNAzol (Invitrogen) according to the recommendations of the manufacturer. Relative telomere lengths were measured by SYBR Green-based (QuantiTect SYBR Green PCR kit; Qiagen, Valencia, CA, USA) qRT-PCR amplification of telomere repeats (T) and single-copy gene *36B4* (S) in a LightCycler 480 Real-Time PCR System (Roche, Foster City, CA, USA). The *36B4* gene was analyzed to normalize for differences in DNA amount between samples. The primers, primer concentrations and thermal cycling profiles were identical to those of Cawthon *et al* [7]. T and S standard curves were generated using serial dilutions (100 to 20 ng) of the DNA from the reference sample. The telomere- and *36B4*-specific qPCRs were carried out in separate plates and a standard curve was produced in each run to allow relative quantification between samples (50 ng per sample). The T/S ratio of one sample relative to that of another corresponds to the relative telomere lengths of their DNA. Since the amount of PCR product approximately doubles during each amplification cycle, the T/S ratio is approximately  $[2^{Ct(\text{telomeres})} / 2^{Ct(36B4)}]^{-1} = 2^{-\Delta Ct}$ . The relative T/S ratio is  $2^{-(\Delta Ct_1 - \Delta Ct_2)} = 2^{-\Delta \Delta Ct}$ .

**CARDIAC DIFFERENTIATION POTENTIAL OF HMSCS DERIVED FROM DIFFERENT SOURCES**

To facilitate the identification of hMSCs in co-cultures with nrCMCs or nrCFBs, these cells were transduced with *enhanced green fluorescent protein* (eGFP) using the vesicular stomatitis virus G protein-pseudotyped self-inactivating human immunodeficiency virus type 1 (HIV-1) vector CMVPRES [8], essentially as described by van Tuyn *et al* [9]. Before being used in co-culture experiments, the eGFP-transduced hMSCs were subcultured for several passages to avoid undesired secondary transductions of nrCMCs or nrCFBs by infectious HIV-1 particles carried over by the hMSCs. Cardiomyogenic differentiation was studied in co-cultures of  $5 \times 10^4$  eGFP-labeled hMSCs and  $5 \times 10^5$  nrCMCs or  $5 \times 10^5$  nrCFBs. As a control group,  $5 \times 10^4$  eGFP-labeled fetal hSFBs were co-incubated with  $5 \times 10^5$  nrCMCs. The eGFP-labeled hMSCs and fetal hSFBs were added to the nrCMCs two days after they had been isolated and put into culture. All experiments described below were conducted using hMSCs from passage 3-6.

*Human-specific immunocytochemical analysis of cardiomyogenic differentiation potential*

Co-cultures of  $5 \times 10^5$  nrCMCs and  $5 \times 10^4$  eGFP-labeled hMSCs or eGFP-labeled fetal hSFBs and co-cultures of  $5 \times 10^5$  nrCFBs with  $5 \times 10^4$  eGFP-labeled hMSCs were stained

with a MAb recognizing the sarcomeric protein  $\alpha$ -actinin (clone EA53; Sigma-Aldrich; dilution 1:400) on day 10 after culture initiation, as previously described [6]. The primary antibody was visualized using Alexa 568-coupled donkey anti-mouse IgG secondary antibodies at a dilution of 1:200. The human lamin A/C-specific MAb mentioned above was used to detect hMSCs in the co-cultures. Lamin A/C staining was visualized with Qdot 655-streptavidin conjugates (Invitrogen) after incubation of the cells with biotinylated goat anti-mouse IgG2b secondary antibodies (Santa Cruz). Nuclei were stained using a 10  $\mu$ g/mL solution of Hoechst 33342 (Invitrogen) in PBS containing 1% FBS. The percentage of eGFP-labeled cells showing positive staining for  $\alpha$ -actinin was determined by analyzing at least 3 cultures (100 cells per culture, at 100x magnification) of at least 4 hMSC isolations per type of hMSC). The presence of well-organized sarcomeres in eGFP-labeled hMSCs was assessed by comparing the  $\alpha$ -actinin staining pattern in these cells with that of the native nrCMCs in each culture.

A fluorescence microscope equipped with a digital camera (Nikon Eclipse, Nikon Europe, Badhoevedorp, The Netherlands) and dedicated software (Image-Pro Plus, Version 4.1.0.0, Media Cybernetics, Silver Spring, MD, USA) were used to analyze data. All co-cultures were treated equally using the same antibody dilutions and exposure times.

#### *Electrophysiological measurements in pharmacologically uncoupled hMSCs in co-culture with nrCMCs*

Whole-cell patch-clamp measurements were performed in co-cultures of  $5 \times 10^4$  eGFP-labeled fetal (amniotic) or adult (adipose) hMSCs and  $5 \times 10^5$  nrCMCs, plated on collagen-coated glass coverslips, at day 10 of culture. To perform single-cell measurements from eGFP-labeled cells in a field of beating nrCMCs, cells were pharmacologically uncoupled by incubation with 180  $\mu$ mol/L of 2-aminoethoxydiphenyl borate (2-APB) (Tocris, Ballwin, MO, USA) for 15 min [6]. This agent blocks gap junctional intercellular coupling by Cx40, Cx43, and Cx45 [10,11]. Whole-cell current-clamp recordings were performed at 25°C using a L/M-PC patch-clamp amplifier (3 kHz filtering) (List-Medical, Darmstadt, Germany). Pipette solution contained (in mmol/L) 10 Na<sub>2</sub>ATP, 115 KCl, 1 MgCl<sub>2</sub>, 5 EGTA, 10 HEPES/KOH (pH 7.4). Tip resistance was 2.0 - 2.5 MW, and seal resistance >1 GW. The bath solution contained (in mmol/L) 137 NaCl, 4 KCl, 1.8 CaCl<sub>2</sub>, 1 MgCl<sub>2</sub>, 10 HEPES (pH 7.4). For data acquisition and analysis pClamp/Clampex8 software (Axon Instruments, Molecular Devices, Sunnyvale, CA, USA) was used. Current-clamp recording were performed in eGFP-labeled cells which were adjacent to 2-4 nrCMCs, and from these cells the data were analyzed and compared between the two different groups.

*Human-specific quantitative reverse transcription-PCR (qRT-PCR) to detect mRNAs associated with pluripotency and cardiac differentiation*

Total cellular RNA was extracted from monocultures of hMSCs ( $n^3_4$  samples from each type of hMSC) and from co-cultures consisting of  $10^5$  hMSCs and  $10^6$  nrCMCs using the RNeasy Mini kit (Qiagen). Oligo (dT)-primed reverse transcription was performed on 2  $\mu$ g of total cellular RNA and the resultant cDNA was used for PCR amplification using SYBR Green. To detect changes in cardiac and pluripotency gene expression levels, the following human-specific primers: gap junction protein, alpha 1 (Cx43/GJA1; QT00012684), vascular endothelial growth factor A (VEGF/VEGFA; QT01682072), GATA-binding protein 4 (GATA-4/GATA4; QT00031997), Nanog homeobox (Nanog/NANOG; QT01844808), octamer-binding protein 3/4 (Oct-3/4/POU5F1; QT00210840), NK2 transcription factor related, locus 5 (Drosophila) (Nkx2.5/NKX2-5; QT00010619), v-kit Hardy-Zuckerman 4 feline sarcoma viral oncogene homolog (c-kit/KIT; QT01844549), natriuretic peptide precursor A (ANP/NPPA; QT00203322), myosin, light chain 2, regulatory, cardiac, slow (MLC2v/MYL2; QT00012999), ISL LIM homeobox 1 (Islet-1/ISL1; QT00000294), troponin I type 3 (cardiac) (cTnI/TNNI3; QT00084917) (all with an annealing temperature of 55°C; all from Qiagen) and myosin heavy chain 7, cardiac muscle, beta (b-MCH/MYH7; forward primer: 5'-TGTGTCACCGTCAACCCTTA-3', reverse primer: 5'-TGGCTGCAATAACAGCAAAG-3'; annealing temperature 63°C; Invitrogen). The expression of the genes of interest was normalized to that of the housekeeping gene *glyceraldehyde-3-phosphate dehydrogenase* (GAPDH, forward primer: 5'-GAA-GGTGAAGGTCGGAGTC-3', reverse primer: 5'-GAAGATGGTGATGGGATTTC-3'; annealing temperature 60°C; Invitrogen). Agarose gel electrophoresis was used to ensure that each primer pair yielded a single PCR product of the expected size. PCR primers were checked for human specificity with the aid of appropriate positive human right atrium and hESC control and negative nrCMC control samples, while rat-specific primers were used to detect expression of the cardiac genes in the nrCMC control samples. Data were analyzed using the  $\Delta$ Ct method.

*Optical mapping to determine CV in co-cultures between nrCMCs and different types of hMSCs*

Action potential propagation was investigated on a whole-culture scale in wells of a 24-well plate by optically mapping using the voltage-sensitive dye di-4-AN-EPPS (Invitrogen). The measurements were performed 10 days after seeding of either  $8 \times 10^5$  nrCMCs (nrCMC monoculture) or  $8 \times 10^5$  nrCMCs plus  $8 \times 10^4$  nrCFBs or  $8 \times 10^4$  hMSCs (nrCMC/nrCFB or nrCMC/hMCS co-cultures) per well ( $n^3_{15}$  cultures per cell type or combination of cell types). Co-cultures were loaded with 16  $\mu$ mol/L di-4-ANEPPS for 30 minutes. After which medium was refreshed and the co-cultures were mapped using the Ultima-L optical mapping setup (SciMedia, Costa

Mesa, CA, USA). Throughout mapping experiments, cultures were kept at 37°C. Optical signal recordings were analyzed using Brain Vision Analyze 0909 (Brainvision Inc, Tokyo, Japan). For more details regarding the optical mapping protocol see Askar *et al* [12]. The CV of all (co-)cultures was determined in a blinded manner.

#### **IN VITRO ANGIOGENESIS ASSAYS**

hMSCs of different origin ( $n^3_5$  isolations for each type of hMSC) were plated on Matrigel (Becton Dickinson) to determine their ability to form capillary-like structures. Ninety microliters of gel matrix solution was applied to each well of a 24-well plate on top of a glass coverslip and the plate was incubated for 1 h at 37°C. After trypsinization,  $1.5 \times 10^4$  cells were suspended in 1 mL of Endothelial Growth Medium-2 (Cambrex IEP, Wiesbaden, Germany) containing 100 ng/mL recombinant human VEGF-A<sub>165</sub> (R&D Systems), plated onto the basement membrane matrix and incubated for up to 24 h at 37°C in 95% humidified air-5% CO<sub>2</sub>. Formation of capillary-like structures was checked every hour. Maximum time of incubation was determined for each type of hMSC. Following culture on the basement membrane matrix, cells were fixed and stained with antibodies specific for smooth muscle myosin heavy chain (smMHC; MAb hSM-V; Sigma-Aldrich, dilution 1:100) and platelet/endothelial cell adhesion molecule-1 (PECAM-1; rabbit PAb M20; Santa Cruz, dilution 1:200). The primary antibodies were visualized with Alexa 568-coupled donkey anti-mouse IgG and Alexa 488-conjugated donkey anti-rabbit IgG (Invitrogen), respectively. All cultures were treated equally using the same antibody dilutions and exposure times, which were based on titration of the antibodies using appropriate positive and negative controls.

#### **DETERMINATION OF CX43 EXPRESSION**

Cx43 protein levels and gene expression were detected in monocultures of hESCMSCs, fetal amniotic hMSCs and adult adipose hMSCs, but also in co-cultures of these cells with nrCMCs or nrCFBs using immunocytology and qRT-PCR, as described earlier. The Cx43-specific rabbit PAb (C6219; Sigma Aldrich, dilution 1:200) was visualized with Alexa 488-conjugated donkey anti-rabbit IgG. Cx43 expression was determined for at least 5 different isolations of each type of hMSCs under the different conditions (100 cells per culture and at least 3 cultures per isolation were analyzed). All cultures were treated equally using the same antibody dilutions and exposure times, which were based on titration of the antibodies using appropriate positive and negative controls.

Western blot analysis was used to quantify Cx43 levels in cultures of hMSCs. Homogenates were made from at least 5 different isolations of hMSCs per source. After determining the protein concentration in each sample using the BCA Protein Assay Reagent (Pierce Biotechnology, Rockford, IL, USA), equal amounts of

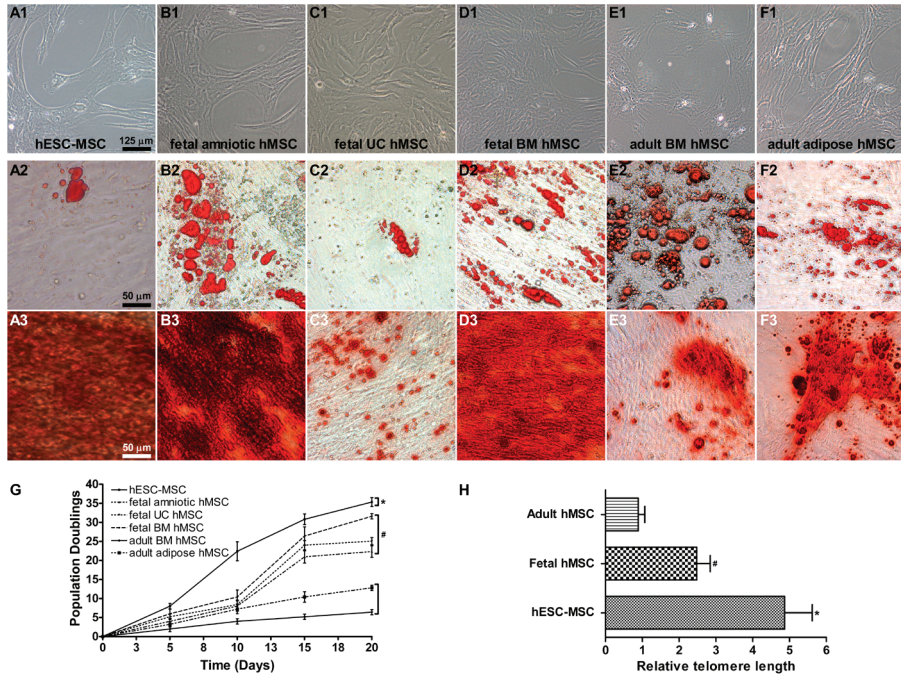
protein were size-fractionated in a 12% NuPage Tris-Acetate gel (Invitrogen) and transferred to a Hybond-P PVDF membrane (GE Healthcare, Waukesha, WI, USA). This membrane was incubated for 1 h with the PAb directed against Cx43 followed by incubation with horse radish peroxidase (HRP)-conjugated goat anti-rabbit secondary antibody (Santa Cruz). To check for equal protein loading, a mouse MAb recognizing the housekeeping protein GAPDH (Chemicon International, Temecula, CA, USA) was used, which was detected by an HRP-conjugated goat anti-mouse secondary antibody (Santa Cruz). Chemiluminescence was induced with the aid of the ECL Advance Western Blotting Detection Kit and caught on Hyperfilm ECL (both from GE Healthcare).

## REFERENCES

1. Trivedi P, Hematti P (2008) Derivation and immunological characterization of mesenchymal stromal cells from human embryonic stem cells. *Exp Hematol* 36: 350-359.
2. Karlsson C, Emanuelsson K, Wessberg F, Kajic K, Axell MZ et al. (2009) Human embryonic stem cell-derived mesenchymal progenitors-Potential in regenerative medicine. *Stem Cell Res.*
3. National Institutes of Health (2002) Guide for the Care and Use of Laboratory Animals.
4. Pijnappels DA, Schalij MJ, van Tuyn J, Ypey DL, de Vries AA et al. (2006) Progressive increase in conduction velocity across human mesenchymal stem cells is mediated by enhanced electrical coupling. *Cardiovasc Res* 72: 282-291.
5. Pittenger MF, Mackay AM, Beck SC, Jaiswal RK, Douglas R et al. (1999) Multilineage potential of adult human mesenchymal stem cells. *Science* 284: 143-147.
6. Pijnappels DA, Schalij MJ, Ramkisoensing AA, van Tuyn J, de Vries AA et al. (2008) Forced alignment of mesenchymal stem cells undergoing cardiomyogenic differentiation affects functional integration with cardiomyocyte cultures. *Circ Res* 103: 167-176.
7. Cawthon RM (2002) Telomere measurement by quantitative PCR. *Nucleic Acids Res* 30: e47.
8. Seppen J, Rijnberg M, Cooreman MP, Oude Elferink RP (2002) Lentiviral vectors for efficient transduction of isolated primary quiescent hepatocytes. *J Hepatol* 36: 459-465.
9. van Tuyn J, Pijnappels DA, de Vries AA, de V, I, van der Velde-van Dijke et al. (2007) Fibroblasts from human postmyocardial infarction scars acquire properties of cardiomyocytes after transduction with a recombinant myocardin gene. *FASEB J* 21: 3369-3379.
10. Bai D, del CC, Srinivas M, Spray DC (2006) Block of specific gap junction channel subtypes by 2-aminoethoxydiphenyl borate (2-APB). *J Pharmacol Exp Ther* 319: 1452-1458.
11. Harks EG, Camina JP, Peters PH, Ypey DL, Scheenen WJ et al. (2003) Besides affecting intracellular calcium signaling, 2-APB reversibly blocks gap junctional coupling in confluent monolayers, thereby allowing measurement of single-cell membrane currents in undissociated cells. *FASEB J* 17: 941-943.
12. Askar SFA, Ramkisoensing AA, Schalij MJ, Bingen BO, van der Laarse A, Atsma DE, Ypey DL, Pijnappels DA (2011) Antiproliferative Treatment of Endogenous Myofibroblasts Prevents the Occurrence of Spontaneous Reentrant Tachyarrhythmias in Rat Myocardial Cultures. *Cardiovasc Res* 90: 295-304.

## SUPPORTING INFORMATION LEGENDS

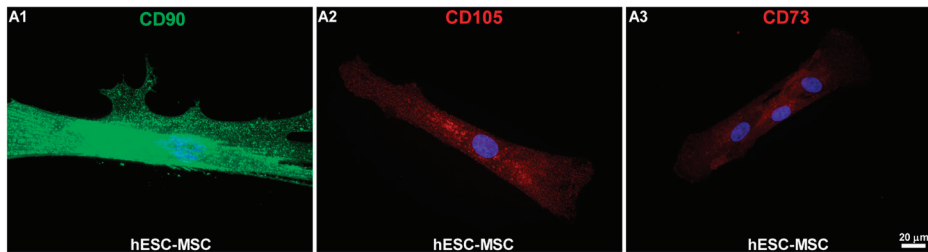
Supplemental Materials and Methods S1. A detailed description of the materials and methods can be found in this supporting information file.



**Supplemental figure S1.** Cellular characteristics of hMSCs. (A1-F1) Bright field images of cultured hMSCs displaying a spindle-shaped morphology. (A2-F2) Presence of oil red O-stained fat vacuoles after adipogenic differentiation. (A3-F3) Calcium depositions after osteogenic differentiation was visualized by alizarine red S staining. (A) hESC-MSC; (B) fetal amniotic hMSC; (C) fetal UC hMSC; (D) fetal BM hMSC; (E) adult BM hMSC; (F) adult adipose hMSC. (G) Growth kinetics of the different types of hMSCs estimated by cumulative population doublings over 20 days ( $^*P < 0.001$  vs fetal hMSCs and adult hMSCs,  $^{\#}P < 0.001$  vs adult hMSCs). (H) Mean relative telomere lengths of hESC-MSCs, all fetal hMSC types and both adult hMSC types ( $^*P < 0.05$  vs fetal hMSCs and adult hMSCs,  $^{\#}P < 0.05$  vs adult hMSCs).

	hESC-MSC	Fetal amniotic hMSC	Fetal BM hMSC	Fetal UC hMSC	Adult BM hMSC	Adult adipose hMSC
CD24	0.30±0.7	NT	NT	NT	NT	NT
CD31	0.0±0.0	0.0±0.0	0.0±0.0	0.0±0.0	0.0±0.0	0.0±0.0
CD34	0.13±0.1	0.0±0.0	0.13±0.1	0.0±0.0	0.17±0.1	0.06±0.0
CD45	0.20±0.4	0.07±0.0	0.10±0.1	0.18±0.1	0.20±0.1	0.6±0.5
CD73	97.6±1.9	95.4±0.8	97.3±1.3	97.7±1.1	96.6±1.4	96.4±0.3
CD90	96.0±1.7	98.2±1.3	96.3±1.5	96.3±3.1	98.2±0.9	94.6±1.8
CD105	94.0±0.9	95±0.9	96.6±0.2	97.4±0.6	96.0±2.8	96.0±0.2
SSEA-4	0.0±0.0	0.0±0.0	0.0±0.0	0.0±0.0	0.0±0.0	0.0±0.0

**Supplemental table S1.** Analysis of surface marker expression. All hMSC types were positive for the established MSC surface markers CD105, CD90 and CD73. They were negative for the hematopoietic, endothelial and embryonic stem cell markers CD45 and CD34, CD31 and SSEA-4, respectively. The hESC-MSCs were also negative for CD24, a protein present on the surface of hESCs. Mean percentages  $\pm$  standard deviations are given; n=6 for each group. NT is not tested.



**Supplemental figure S2.** Immunocytological characterization of hESC-MSCs for MSC surface markers. Immunostaining of hESC-MSCs for CD90, CD105 and CD73 (A1-A3) showed that these cells were positive for these established MSC surface markers.

	Nkx2.5	GATA-4	ANP	MLC2v	Cx43	VEGF	Islet-1	c-kit
hESC-MSC	6.15±1.2*	5.77±0.6#	2.97±0.1†	12.0±0.6†	9.13±0.9#	1.18±0.3	0.43±0.1*	0.53±0.2#
Fetal amniotic hMSC	7.26±0.4#	ND	1.56±0.1*	ND	3.94±0.5*	3.85±0.3*	0.35±0.1#	0.75±0.2
Fetal UC hMSC	ND	5.79±1.4#	1.04±0.1	ND	2.72±0.2#	2.32±0.1†	0.50±0.1†	0.36±0.1*
Fetal BM hMSC	ND	ND	3.73±0.1†	ND	1.97±0.3#	0.93±0.1	6.13±1.9	6.13±1.9†
Adult BM hMSC	ND	ND	2.07±0.4#	ND	1.03±0.3	1.44±0.8*	ND	0.84±0.3
Adult adipose hMSC	ND	ND	5.18±1.5#	ND	1.22±0.2	11.7±1.8*	ND	5.71±1.0#

**Supplemental table S2.** qRT-PCR analysis to detect mRNAs associated with cardiac differentiation. Indicated is the fold change in the expression of cardiac genes in hMSCs cultured alone or together with nrCMCs. # $P < 0.05$  vs hMSC monoculture; \* $P < 0.01$  vs hMSC monoculture; † $P < 0.001$  vs hMSC monoculture; ND is not detected.